

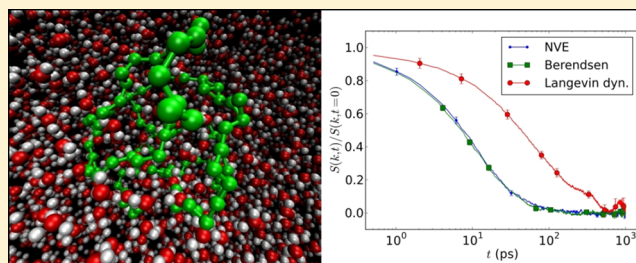
Effects of Temperature Control Algorithms on Transport Properties and Kinetics in Molecular Dynamics Simulations

Joseph E. Basconi and Michael R. Shirts*

Department of Chemical Engineering, University of Virginia, Charlottesville, Virginia 22904-4741, United States

S Supporting Information

ABSTRACT: Temperature control algorithms in molecular dynamics (MD) simulations are necessary to study isothermal systems. However, these thermostating algorithms alter the velocities of the particles and thus modify the dynamics of the system with respect to the microcanonical ensemble, which could potentially lead to thermostat-dependent dynamical artifacts. In this study, we investigate how six well-established thermostat algorithms applied with different coupling strengths and to different degrees of freedom affect the dynamics of various molecular systems. We consider dynamic processes occurring on different times scales by measuring translational and rotational self-diffusion as well as the shear viscosity of water, diffusion of a small molecule solvated in water, and diffusion and the dynamic structure factor of a polymer chain in water. All of these properties are significantly dampened by thermostat algorithms which randomize particle velocities, such as the Andersen thermostat and Langevin dynamics, when strong coupling is used. For the solvated small molecule and polymer, these dampening effects are reduced somewhat if the thermostats are applied to the solvent alone, such that the solute's temperature is maintained only through thermal contact with solvent particles. Algorithms which operate by scaling the velocities, such as the Berendsen thermostat, the stochastic velocity rescaling approach of Bussi and co-workers, and the Nosé-Hoover thermostat, yield transport properties that are statistically indistinguishable from those of the microcanonical ensemble, provided they are applied globally, i.e. coupled to the system's kinetic energy. When coupled to local kinetic energies, a velocity scaling thermostat can have dampening effects comparable to a velocity randomizing method, as we observe when a massive Nose-Hoover coupling scheme is used to simulate water. Correct dynamical properties, at least those studied in this paper, are obtained with the Berendsen thermostat applied globally, despite the fact that it yields the wrong kinetic energy distribution.



1. INTRODUCTION

Temperature control algorithms are an important component of many molecular dynamics simulations. Using a method to enforce constant temperature is necessary to compare simulation results with laboratory experiments conducted at constant temperature and either constant pressure or volume.^{1–3} Precise control of the temperature is necessary when studying temperature-dependent properties and phenomena,^{4,5} as a constant energy simulation may not have either the correct average kinetic energy or correct distribution of kinetic energies. Controlling the temperature can prevent the system from heating significantly over long time scales (though good integration algorithms should already minimize this drift) and can improve the efficiency of conformational sampling in some cases.⁶

A molecular dynamics thermostat couples a fictitious heat bath to the system or some portion of the system, such that the time-averaged instantaneous kinetic energy of the coupled degrees of freedom corresponds to a target temperature. This coupling is commonly achieved by altering Newton's equations of motion or the particle velocities themselves during the simulation, so that the kinetic energy is steered toward its target. For a thermostat to be entirely consistent with the

canonical ensemble, it should generate total energies according to the Boltzmann distribution for that system and generate kinetic energies consistent with the Maxwell–Boltzmann distribution. Additionally, the dynamics should be ergodic, meaning all states with the same energy are visited with equal probability in the long time limit. However, this thermodynamic specification of the correct distribution of energies for the NVT ensemble does not define what the dynamics of the system should be. There are many different equations of motion to choose from for a classical molecular system that result in the same correct thermodynamics.

If an accurate representation of transport properties or other dynamical quantities is required, then the thermostat should, besides just maintaining the correct kinetic energy distribution, operate in such a way that minimally disturbs the Newtonian dynamics. Since the equations of motion are altered when using a thermostat, some disturbance of the dynamics must occur, though the extent of such a disturbance is in general not known.

Received: February 13, 2013

However, some common algorithms are known to cause significant dampening of the energy fluctuations or dynamics of the system. As the first problem of obtaining the correct energy fluctuations is generally well understood,⁷ this study deals primarily with the latter problem. Specifically, we investigate the effects of different temperature control schemes on basic dynamical properties relevant to experiments by studying three test systems: a pure solvent, a solvated small molecule, and a solvated polymer chain. These properties illustrate the effects on dynamic processes that occur over different time scales. The tested temperature control schemes include different thermostats, coupling strengths, and degrees of freedom to which the thermostat is applied.

Section II of this paper briefly reviews the different thermostat algorithms we consider as well as related research on how temperature control influences dynamics. In Section III we describe the details of the simulations and the transport properties calculated. In Sections IV and V we discuss the effects of the various temperature coupling schemes, particularly with regard to the dynamics, and consider implications of these findings.

2. BACKGROUND

2.1. Thermostat Algorithms. A variety of methods have been developed to perform isothermal MD simulations. Here we briefly describe the thermostat algorithms tested in this study and particular aspects of their implementation in the GROMACS simulation package used throughout the work.⁸ Conceptually, the use of any thermostat is analogous to coupling a fictitious heat bath to the system in order to maintain the average temperature T at some target T_0 . This heat bath is applied to a given particle i , either by directly altering the particle's velocity or by modifying Newton's equation of motion:

$$m_i \frac{d^2 \mathbf{r}_i}{dt^2} = \mathbf{F}_i(\mathbf{r}_i) \quad (1)$$

In the absence of temperature control, the system evolves classically according to eq 1 and has the microcanonical (NVE) distribution of energies. This ensemble provides the “true” dynamics, i.e. classical Newtonian dynamics for a system described by a given force field, at the accuracy level determined by the force calculations and integration algorithm used. In this study we therefore compare dynamical properties obtained from Newtonian (constant energy) dynamics with those from NVT simulations with different types of temperature control.

The coupling strength τ_T determines how strongly the heat bath is applied to the system or how quickly deviations in T are “pulled back” to T_0 . While the physical meaning of τ_T varies depending on the algorithm, in general T is more tightly controlled as $\tau_T \rightarrow 0$ and less tightly controlled as τ_T increases, with the system approaching the NVE ensemble in the limit $\tau_T \rightarrow \infty$. If an algorithm implements the canonical distribution correctly, τ_T will not affect the distribution of kinetic energies sampled, only the rate of change of the instantaneous kinetic energy.

Among the six thermostat algorithms that we test are methods which randomize particle velocities in order to control the temperature. In the Andersen thermostat, at each time step in the simulation a subset of atoms are randomly selected and reassigned new velocities chosen from the Maxwell–Boltzmann

distribution corresponding to the target temperature.⁹ Each particle experiences stochastic collisions which occur on average every τ_T and evolves according to Newton's equation of motion in between collisions. $\Delta t/\tau_T$ (where Δt is the time step) is the probability that any given particle is selected for velocity reassignment at a given time step or, effectively, the size of the subset of particles to be randomized at a given step. Tighter temperature control is obtained when the chance for a particle's velocity to be randomized is large, corresponding to low values of τ_T . We also test a “massive Andersen” thermostat in which the velocities of all particles are randomized at intervals of τ_T . Both Andersen schemes generate energy distributions consistent with the canonical ensemble^{7,10} and require no direct modification of the integration equations themselves.

Another stochastic approach to temperature control uses the Langevin equation of motion to describe the evolution of the system⁸

$$m_i \frac{d^2 \mathbf{r}_i}{dt^2} = -m_i \xi_i \frac{d\mathbf{r}_i}{dt} + \mathbf{F}_i(\mathbf{r}_i) + \hat{\mathbf{r}}_i \quad (2)$$

where ξ_i is a friction constant, typically though not necessarily the same for all particles, and $\hat{\mathbf{r}}_i$ is a stochastic noise term proportional to ξ_i and the target T_0 . Here τ_T is inversely proportional to the friction constant. Thus, as $\tau_T \rightarrow 0$ the temperature is more tightly controlled due to both greater friction (removing more energy) and stochastic noise (adding more energy) in the system. With a carefully chosen coupling strength, Langevin dynamics may be used to approximate solvent interactions in an implicit solvent environment, as the stochastic forces on the molecules simulated in vacuum represent the friction and random thermal noise of collisions with an explicitly represented solvent.⁶ Langevin dynamics has been shown to be ergodic for a wide range of systems.¹¹

In contrast to approaches that randomize the velocities, the temperature may be controlled by scaling the velocities at regular intervals. Here the equation of motion is

$$m_i \frac{d^2 \mathbf{r}_i}{dt^2} = -m_i \gamma \frac{d\mathbf{r}_i}{dt} + \mathbf{F}_i(\mathbf{r}_i) \quad (3)$$

which is of a similar form as eq 2, only with no stochastic noise term, and a term γ that is not restricted to positive values (as is the friction constant in eq 2) and is usually the same for all degrees of freedom. γ as well as the velocity scaling factor, λ , are both functions of τ_T^{-1} ; therefore, the velocities are scaled more significantly to achieve tighter temperature control when $\tau_T \rightarrow 0$. The magnitude of the velocity scaling is generally low, however, because τ_T typically describes the time constant for relaxation of the ensemble-averaged temperature (or kinetic energy) of the entire system to the target. With a sufficiently large number of degrees of freedom added together, the temperature varies slowly, and therefore the required velocity scalings are small.

The original “weak coupling” scaling algorithm devised by Berendsen uses an exponential decay of the temperature¹²

$$\frac{dT}{dt} = \tau^{-1} [T_0 - T(t)] \quad (4)$$

where the time constant $\tau = 2C_V\tau_T/(N_f k_B)$, with C_V representing the constant volume heat capacity, k_B representing Boltzmann's constant, and N_f representing the number of degrees of freedom of the system. However, this approach

yields an energy distribution with lower variance than the distribution of the true canonical ensemble, because it disproportionately samples kinetic energies closer to T_0 than would be observed in the Maxwell–Boltzmann distribution.⁷ Bussi and co-workers developed an extension to the method which addresses this distribution problem.¹³ We refer to this method as a “stochastic rescaling” thermostat to distinguish it from the other velocity scaling algorithms, as it not only rescales the velocities similarly to Berendsen but also includes a stochastic term in the equation describing the decay of the kinetic energy K

$$dK = (K_0 - K) \frac{dt}{\tau_T} + 2 \sqrt{\frac{K_0}{N_f}} \frac{dW}{\sqrt{\tau_T}} \quad (5)$$

where K_0 is the kinetic energy corresponding to the target temperature T_0 such that $K_0 = (N_f k_B T_0)/2$, the instantaneous temperature T is related to the instantaneous K by the same relationship, N_f is again the number of degrees of freedom, and dW is a Wiener process noise term. Including this stochastic noise yields the correct energy fluctuations for the canonical ensemble.

The widely used Nosé–Hoover and Nosé–Hoover-chains thermostats utilize an extended system to relax the temperature to T_0 in an oscillatory manner.^{14–16} The Nosé–Hoover method is also a scaling thermostat, as the velocities are scaled by a variable $p_\eta = Q d\eta/dt$ describing the momentum of a heat bath η coupled to particle i and the instantaneous temperature of the system, in the following coupled equations of motion for \mathbf{r} and η

$$\begin{aligned} \frac{d^2 \mathbf{r}_i}{dt^2} &= \frac{\mathbf{F}_i(\mathbf{r}_i)}{m_i} - \frac{p_\eta}{Q} \frac{d\mathbf{r}_i}{dt} \\ \frac{d^2 \eta}{dt^2} &= \frac{T - T_0}{Q} \end{aligned} \quad (6)$$

where Q is the equivalent of the mass of the heat bath. The equations give the correct kinetic energy distribution for any arbitrary choice of Q , though lighter masses lead to faster oscillatory behavior. In the GROMACS implementation, $Q = (\tau_T^2 T_0 N_f)/(4\pi^2)$, where N_f is the number of degrees of freedom to which the thermostat is applied, and the coupling strength τ_T describes the period of oscillations of kinetic energy transferred between the system and the heat bath. With Nosé–Hoover integration the conserved quantity can be obtained from an extended Lagrangian and is a function of η , p_η and Q .

The Nosé–Hoover thermostat has a drawback in that it is provably nonergodic and therefore does not sample the canonical ensemble for certain systems,¹⁰ though it appears to be statistically indistinguishable from the canonical distribution for molecular systems when particle number is in the hundreds or larger.⁷ Martyna et al. proposed an extension, known as the Nosé–Hoover-chains method, in which the heat bath η_1 in contact with the system is itself in contact with a chain of N_C additional heat baths.¹⁶ The equations of motion are therefore coupled to a chain of N_C additional bath variables increasing the computation time and complexity but increasing the ergodicity of the dynamics by increasing the available phase space of the dynamics.

Thermostats (like Berendsen, Nosé–Hoover, and Bussi’s algorithm) which scale the velocities based on a single bath variable shared between all degrees of freedom can leak kinetic

energy from high frequency modes into lower frequency modes, especially the translational or rotational degrees of freedom which are decoupled from the rest of the system. This is another possible way that the ergodic assumption can break down when dynamics are modified by thermostats. This problem most egregiously manifests itself in the “flying ice cube” problem,¹⁷ where all the kinetic energy available to the system moves into translation and rotational motion. The general solution is to subtract out the kinetic energy of these degrees of freedom. There is some evidence that kinetic energy may accumulate in other low frequency vibrational modes,^{17,18} but the general scope of the problem appears not to have been studied significantly since then, remaining an open question. Bussi et al. did find that using their algorithm, the phonon distribution of ice remained the same between NVE and NVT simulations,¹³ indicating that at least in standard usage, this problem may not be significant for stochastic velocity rescaling.

2.2. Thermostats and Dynamics. As described above, different thermostat algorithms have various influences on the classical equations of motion. These influences lead to different effects on the dynamics of a simulation, which we aim to quantify in this study. The dampening of dynamical processes such as diffusion can be attributed to disturbances of the natural time correlations of a particle’s velocity, which can be identified by calculating the velocity autocorrelation function (ACF). While any algorithm which alters the classical equations of motion will have some effect on velocity time correlations and thus dynamical properties, these effects can be negligible depending on the algorithm and the coupling strength at which the thermostat is applied. Observed dampening in an ensemble- or time-averaged transport property is indicative of consistent rapid decorrelation of velocities, throughout the system or over the course of the simulation.

Thermostats which operate by randomizing velocities, such as the Andersen and Langevin dynamics methods, significantly disturb velocity time correlations if the coupling is sufficiently strong. The decorrelation of velocities is an obvious consequence of velocity randomization, whether by randomly reassigning velocities in the case of Andersen or by imposing stochastic forces on the particles in the case of Langevin dynamics. While in the limit of weak coupling (large τ_T), the Andersen thermostat is expected to have a small effect on system dynamics, it has still been advised not to use such a stochastic method when studying dynamical properties.¹⁰

We hypothesize that typical implementations of velocity scaling thermostats generally preserve the correct velocity time correlations, which should be reflected in the dynamical properties we measure. This assumes the scaling algorithm is implemented “globally”, i.e., by coupling the scaling factor or heat bath variable for each particle to the system’s overall kinetic energy (or temperature). As previously mentioned, the overall kinetic energy typically exhibits relatively slow fluctuations at equilibrium, and therefore only small changes to the velocities should be necessary to relax this quantity to its target. However, coupling a more rapidly fluctuating energy (e.g., an individual particle’s energy) to the scaling factor or heat bath variable of a given particle could lead to larger changes in the velocity, which could in turn affect the velocity time correlations.

This sort of coupling is used in “local” implementations of a thermostat, which apply independent thermostats to individual molecules or atoms that respond to the kinetic energies of the individual particles, not the total kinetic energy. They can even

be applied to individual degrees of freedom,¹⁹ although single atoms are the smallest units that can be acted upon individually in GROMACS. The independent coupling of all atoms or degrees of freedom individually is often referred to as a massive thermostat scheme. This use of “massive” is different than for the previously mentioned massive Andersen algorithm, which stochastically randomizes all velocities simultaneously, independently of the kinetic energies of both individual particles and the overall system. Similarly, the conventional Andersen thermostat is not local by this definition because alterations of particle velocities are again independent of the kinetic energy. Langevin dynamics is also not local in the same way as the scaling-based methods; although the frictional term is proportional to the particle velocity, the random term is not, and the friction term can never increase the velocity. Massive Nosé-Hoover coupling is sometimes used in practice, particularly for ab initio molecular dynamics, as it can be an effective approach for equilibrating a simulation and improving ergodicity.^{19,20} Finally, we note that using an extremely strong coupling for a global velocity scaling thermostat (corresponding to shorter time scales than examined in this paper) could possibly cause rapid velocity decorrelation as well, if imposing an overly fast relaxation of the system’s kinetic energy to the target led to sufficiently large changes in the velocities.

We have thus identified two different factors which could rapidly decorrelate velocities and lead to dampened dynamics: the direct randomization of velocities and the scaling of velocities if implemented in a local coupling scheme or with very strong coupling, such that velocities change rapidly when the kinetic energy deviates from its target. These factors will be further discussed in light of simulation results obtained using various thermostat schemes.

2.3. Thermostat Schemes which Treat Separate Groups of Atoms Differently. In addition to the effects of the thermostat algorithm, we are also interested in how a solvated molecule’s dynamics may be affected if temperature coupling is applied only to the solvent. This scheme may be viewed equivalently as using separate thermostats for the solute and solvent, with infinite and finite coupling strengths, respectively. Lingenheil and co-workers have termed this the “noninvasive” coupling scheme and have also considered a minimally invasive scheme in which τ_T applied to the solute is much larger than the time constant describing the relaxation of the separately coupled solute’s T to its steady state, as measured from simulation.²¹ Note that these schemes could be implemented either “globally” or “locally”, in the sense that the terms are used above; the separate temperature control applied to the solvent or any subsystem may involve a single thermostat for each particle in the subsystem or alternatively independent thermostats for each particle.

The non- and minimally invasive schemes as well as a commonly used approach in which separate thermostats are applied with a small τ_T for both subsystems^{22–24} are well suited for systems with inhomogeneous rates of heating. In these cases, applying a single thermostat to the entire system can give rise to nonuniform temperature distributions, otherwise known as the “hot solvent-cold solute” problem, due to the fact that kinetic energy can flow between the different degrees of freedom through the heat bath variables and create a steady state distribution inhomogeneous in temperature. Using a non- or minimally invasive coupling scheme can circumvent this problem and avoid artifacts in the solute dynamics associated with the inhomogeneous heating, as long as the heat transfer

rate due to molecular collisions between solvent and solute is non-negligible.

In principle, the most physically realistic way to control a system’s temperature is to do so exclusively through thermal contact with the surroundings, using the unaltered Newton’s equation of motion. If the system is sufficiently large, the solvent will act as a perfect heat bath for the solute, and the solute must therefore have a canonical distribution of energy.^{21,25} This type of temperature control would be difficult to achieve with current MD simulations, however. A non-periodic box whose edges were in physical contact with walls of a fixed temperature would represent a truly physical thermal bath, but in most cases the number of solvent particles required to prevent the edges from influencing the solute would be prohibitively large. Alternatively, a thermostat might be applied only to molecules at the edges of a periodic box, but again very large system sizes would be required to prevent solutes from being directly affected by the thermostatted regions, particularly if multiple solutes are included. This scenario also would introduce nonphysical, anisotropic heat source/sink terms into the system.

The noninvasive coupling scheme in which only the solvent is thermostatted can be seen as the next best approach if the integration is sufficiently accurate that the solute’s energy does not drift significantly in the absence of direct temperature control. A solute with unaltered dynamics is coupled to a heat bath (in this case, the bulk solvent) through molecular collisions, not through a extradimensional variable (velocity scaling methods), through collisions with phantom particles (the Andersen variants), or through both (Langevin dynamics). By thermalizing only the solvent, we are closer to the “natural” dynamics of a solute in contact with a solvent, which is itself in contact with the heat reservoir. If heat is produced as a result of molecular motion, it may lead to spatially inhomogeneous temperature transients through the system; but of course this is closer to “natural” heating behavior of the system. In this study we test the extent to which removing temperature coupling of the solute can also reduce artifacts in its dynamics due to the thermostat algorithm.

2.4. Previous Findings. This paper aims to draw consistent comparisons between the effects of different temperature coupling schemes on common dynamical properties. Bussi and co-workers have considered the dynamics of homogeneous systems using their stochastic velocity rescaling thermostat used for temperature control. They found that the diffusion of TIP4P water using this thermostat with a range of coupling strengths agreed with the result of an NVE simulation. The thermostat also yielded the correct features of the vibrational spectrum of hydrogen atoms in ice.¹³ In simulations of a Lennard-Jones fluid it was also found that diffusion was independent of τ_T using stochastic velocity rescaling but dampened with Langevin dynamics at low τ_T .¹¹ We expect to see similar trends for pure fluid self-diffusion and solute diffusion in our study and hypothesize that other dynamical properties will be affected similarly.

Another study assessed the “efficiency” of different thermostats by comparing the error in the dynamics resulting from the thermostat to the characteristic time for equilibration of the kinetic energy.²⁶ In simulations of a homogeneous system, stochastic velocity rescaling and a modified Nosé-Hoover approach that included stochastic influences were both found to be more efficient thermostats than Langevin dynamics, and they perturbed the dynamics to a lesser extent. The dynamics of

a pure SPC/E water system were considered in another study, which measured the power spectra of fluctuating energies.¹⁸ It was found that weak ($\tau_T > 1$ ps) Berendsen coupling yielded power spectra of potential energy fluctuations which matched those from the NVE ensemble, while strong Berendsen coupling led to significant deviations at low frequencies. Another study considered protein dynamics through the power spectra of the velocity ACFs of $\alpha - C$ atoms and the ACFs of dihedral fluctuations, using different temperature control methods: Langevin dynamics, a global Nosé-Hoover thermostat, and global as well as local Nosé-Hoover-chains algorithms.¹⁹ The various Nosé-Hoover and Nosé-Hoover-chains methods yielded ACFs with the same qualitative features as the NVE results (though peak intensities varied), but these dynamical features were not preserved using Langevin dynamics.

Dissipative particle dynamics (DPD) is another common simulation approach.²⁷ As with Langevin dynamics, it includes friction and noise terms that when properly balanced provide a means for temperature control. However, with DPD these forces are applied to particle pairs rather than to individual particles, thus preserving the total linear momentum of each pair. Goga and co-workers recently applied the thermostat component of DPD to various molecular systems using an implementation in which the system is evolved classically for one step, followed by an impulsive application of friction and noise.²⁸ They compared how diffusion was affected by Langevin dynamics versus this DPD thermostat approach, with the pairwise forces applied isotropically, or perpendicular or parallel to the direction of the velocity difference of a given particle pair. In each of these three cases, diffusion using DPD was strongly dependent on the effective friction rate (related to our coupling strength τ_T), despite the modification of the equations of motion to conserve pairwise linear momentum. Lowe also showed that the DPD approach enhances the shear viscosity, which is useful when applying DPD with smoothed potentials with artificially low viscosity to make such simulations more physical, but in our context, is more problematic—DPD modifies and slows the underlying Newtonian dynamics.²⁹ Existing results for DPD are not entirely unambiguous; in one study of polymer brushes under fluid flow, the correct dynamic fluctuations of the polymers were obtained with DPD temperature control but not with Langevin dynamics, reportedly because of the momentum conservation of the former.³⁰ However, it is clear that DPD thermostats do not inherently preserve transport properties.

A thermostat's impact on the thermodynamic ensemble can also be important in order to efficiently sample complex systems and obtain the correct distribution of conformations. It has been rigorously shown that the Berendsen thermostat does not generate the true canonical ensemble, with too narrow a distribution of kinetic, potential, and total energies.⁷ An incorrect ensemble of energies can lead to systems being trapped in local energy minima, as seen in one study which found the time required for a protein to fold increased with strong Berendsen coupling.³¹ In replica exchange molecular dynamics simulations, the Berendsen thermostat has been shown to alter the distribution of folded and unfolded conformations of different peptides at low temperatures.^{32,33} Kinetic processes which depend on the thermodynamics of the system can be similarly affected. Lingenheil and co-workers simulated a peptide with separate strongly coupled thermostats for the solute and solvent as well as with their minimally

invasive scheme in which the solute coupling is relaxed.²¹ Using the Berendsen thermostat for the solute, the peptide backbone exhibited dampened dynamics (as seen in a lower flip rate of the torsional angles) with strong coupling, relative to the minimally invasive scheme. No dampening was observed with the Nosé-Hoover thermostat applied in the same manner, suggesting that the correct energy fluctuations (which are suppressed by the Berendsen method) are necessary to allow the energy barrier crossings associated with certain kinetic processes.

These studies illustrate that the appropriate temperature control scheme largely depends on the processes or phenomena of interest. In this study, we test the commonly used thermostats and coupling strategies described above, in order to provide a consistent comparison of how various thermostatting schemes affect transport properties and the thermodynamic ensemble, which can in turn affect kinetics. Understanding the extent to which thermostats may alter these aspects of a simulation should help improve the analysis of MD studies at constant temperature.

3. METHODS

3.1. Simulation Details. We simulate three test systems, a pure solvent, a solvated small molecule, and a solvated uncharged polymer chain with a variety of temperature control schemes. Water was used as the solvent in each system. The small molecule system includes a single united-atom (UA) methane, while the polymer system includes a single coarse-grained chain comprised of $N = 100$ united atom monomers. Table 1 provides additional details on the systems, which are

Table 1. Simulation Details for Test Systems

system	N_{solvent}	box length (Å)	number of sim.	length (ns) of sim.
pure solvent	895	3.0258	1	10
solvated UA-methane	893	2.9996	1	200
solvated polymer chain	10192	6.7500	15	1

studied in a cubic box with periodic boundary conditions, and the number and length of simulations. The GROMACS molecular dynamics package (a prerelease version of GROMACS 4.6) is used for these studies.⁸ We use the standard 6-12 Lennard-Jones potential to describe all van der Waals interactions and the TIP3P water model for the solvent, with water model constraints maintained using the SHAKE algorithm.^{34,35} The Lennard-Jones radius and well depth for the UA-methane are obtained from the OPLS force field.³⁶ For the polymer chain, these parameters are obtained from the TraPPE united atom force field for hydrocarbons.³⁷ For the middle and terminal monomers we use the parameters for united-atom CH_2 and CH_3 in an alkane, respectively. While the TraPPE force field treats bonds with fixed lengths and bending and torsional potentials, we use only a harmonic potential to describe the bonds, with an equilibrium distance and spring constant corresponding to aliphatic sp^3 hybrid carbons.³⁸ This simplified model leads to a very flexible chain which does not accurately describe a real alkane but serves as a simple model for measuring the effects of thermostats on collective polymer dynamics.

For all systems and integrators the simulation time step is 2 fs. The Particle-mesh Ewald (PME) method is used to calculate

Coulombic forces, along with a switch potential with $r_{\text{switch}} = 0.89$ nm and $r_{\text{Coulomb}} = 0.9$ nm. van der Waals forces are also treated with a switch potential with $r_{\text{vdw-switch}} = 0.8$ nm and $r_{\text{vdw}} = 0.9$ nm, and the neighbor list cutoff is $r_{\text{list}} = 1.1$ nm. We use the velocity Verlet integration scheme³⁹ for all simulations except when Langevin dynamics provides the temperature control, where the leapfrog integration scheme⁴⁰ is used.

We simulate each system with six different thermostats with target temperature $T_0 = 300$ K as well as the NVE ensemble (or coupling with $\tau_T \rightarrow \infty$). For each thermostat we test the coupling strengths $\tau_T = 0.1, 1.0$, and 10.0 ps, values which were kept constant for the sake of consistency, despite the somewhat different physical meaning of τ_T for the various algorithms. In the small molecule and polymer systems, for each thermostat and τ_T we consider the two coupling schemes described previously, in which the thermostat either is applied to the entire system or applied only to the solvent particles, as proposed in the “noninvasive” scheme of Lingenheil and co-workers.

The tested thermostats include three “velocity randomizing” algorithms: the Andersen thermostat, a massive Andersen thermostat which randomizes the velocities of all particles, and Langevin dynamics. We also test three “velocity scaling” algorithms: the Berendsen thermostat, Bussi and co-workers’ stochastic rescaling thermostat, and the Nosé-Hoover thermostat. For the simulations of the pure solvent, we also evaluated the Nosé-Hoover chains approach with $N_C = 50$ chains. However, the results are statistically indistinguishable from those obtained using only a single bath variable, and therefore we report only the Nosé-Hoover results here.

For every system, the initial configurations were obtained by running an energy minimization followed by MD simulation for 1 ns with constant temperature and pressure (stochastic velocity rescaling thermostat with $\tau_T = 0.1$ ps and $T_0 = 300$ K; Berendsen barostat with $\tau_p = 0.5$ ps and $P_{\text{ref}} = 1$ bar). For the NVE simulations, initial kinetic energies were chosen so that the steady state average kinetic energy was within 1% of the target NVT kinetic energy. For the pure solvent and small molecule systems, all simulations are started from the same initial configuration, followed by a 100 ps equilibration period, long enough for the chosen thermostat to determine the dynamics.

As shown in Table 1, a single extended simulation is used to calculate the pure solvent and small molecule transport properties. Consecutive sections of the trajectories are analyzed because the properties are not significantly correlated from one section to another. Because the dynamics of the polymer chain evolve more slowly, however, we analyze 15 independent 1 ns simulations to avoid biased estimates of means and uncertainties due to correlated samples. Prior to collecting data for each independent polymer simulation, we ran for 200 ps with stochastic velocity rescaling ($\tau_T = 0.1$ ps) to obtain a polymer configuration uncorrelated with the previous structure, as measured by the root mean squared deviation (RMSD) of the configuration relative to an initial structure. This was followed by 100 ps of equilibration with the desired temperature coupling scheme, to allow its effects on the dynamics to become dominant.

3.2. Dynamical Properties. We measure a number of different transport properties to investigate how dynamics occurring over different time scales are affected by temperature control. The translational diffusion constant of a given molecule

i is calculated from its average mean square displacement (MSD) using the following Einstein relation:⁴¹

$$2tD = \frac{1}{3} \langle |\mathbf{r}_i(t) - \mathbf{r}_i(0)|^2 \rangle \quad (7)$$

We evaluate the MSD of the molecule’s center of mass, averaged over time for all systems as well as over the ensemble of molecules for the pure water system. For the pure water and small molecule, D is measured from the slope of the MSD between $t = 4$ and 20 ps, a region which avoids the ballistic regime at short times and noise due to insufficient sampling at long times.⁴² We average the diffusivities measured from consecutive 100 ps sections of the 10 ns trajectory to obtain our overall estimate of D and estimate the standard error by bootstrapping the standard deviation of the mean (using 1000 bootstrap samples).

For polymer diffusion, to avoid correlated samples we calculate only one MSD for each independent 1 ns trajectory and average the diffusivities from these 15 sections to obtain D . Error estimates for the polymer diffusivities are comparable with those of the other systems despite the smaller number of samples, because analyzing longer trajectories reduces the uncertainty in each MSD curve.

For the pure solvent, we also calculate the rotational correlation time, τ_α , describing the time required for a water molecule to rotate about a given axis α . Here we consider rotation about the axis normal to the plane spanned by the two O–H bonds. The correlation time is estimated by integrating the following rotational correlation function, calculated from consecutive 100 ps sections of the trajectory

$$C_1^\alpha(t) = \langle P_1(\mathbf{e}^\alpha(t) \cdot \mathbf{e}^\alpha(0)) \rangle \quad (8)$$

where P_1 is a first order Legendre polynomial, and \mathbf{e} is the unit vector along the α axis. Because the tail of this autocorrelation function converges slowly, we estimate the area from $t = 0$ to 5 ps by direct integration of eq 8, and from $t = 5$ to 20 ps by integrating the following exponential fit to the data:⁴³

$$C_1^\alpha(t) = \exp^{-t/\tau_\alpha} \quad (9)$$

As before, we estimate τ_α by taking the mean of the correlation times from the 100 ps subsections of the trajectory and its associated error by bootstrapping the standard deviation of the mean (1000 bootstrap samples).

The shear viscosity of the pure fluid is calculated using the Green-Kubo relation⁴⁴

$$\eta = \frac{V}{k_B T} \int_0^\infty \langle P_{\alpha\beta}(t_0 + t) P_{\alpha\beta}(t_0) \rangle_{t_0} dt \quad (10)$$

where T is the average instantaneous temperature, and $P_{\alpha\beta}$ are the off-diagonal elements of the pressure tensor, and the integrand is averaged over multiple reference times t_0 . The ACF of $P_{\alpha\beta}$ is calculated from $t = 0$ to 1.8 ps. To integrate this slowly converging function, we estimate the area under the curve directly from $t = 0$ to 0.4 ps, and the area under an exponential fit to the data from $t = 0.4$ to 1.8 ps. We evaluate eq 10 for each of the three off-diagonal elements of the pressure tensor, for the four consecutive 2500 ps sections of the trajectory, and estimate η and the associated error by averaging these 12 data points and bootstrapping the standard deviation of the mean (1000 bootstrap samples). Error estimates did not vary significantly with the length of the trajectory used to calculate the ACF; however, a slight minimum in the standard error was obtained

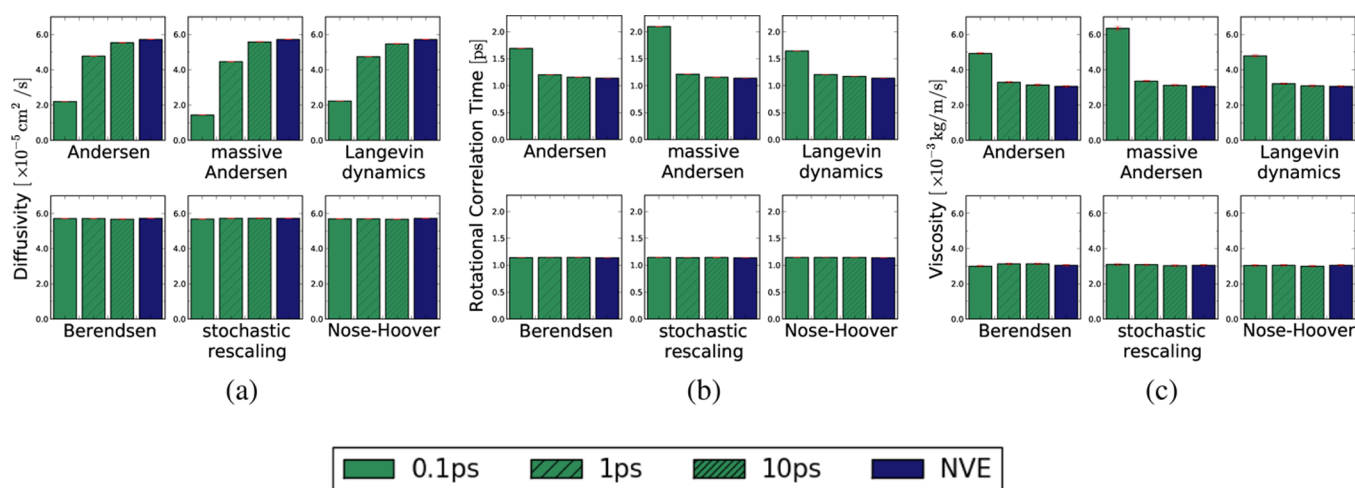


Figure 1. Self-diffusivity (a), rotational correlation time (b), and shear viscosity (c) of pure TIP3P water system with various types of temperature control. Velocity randomizing thermostats (upper figures) with strong coupling slow the diffusion and increase the correlation time and viscosity, while the velocity scaling algorithms do not affect the kinetic properties.

using 2500 ps sections. It should be noted that while nonequilibrium methods are often used to compute the shear viscosity with good accuracy,⁴⁴ the Green-Kubo relation is more appropriate for studying how the viscosity at equilibrium is affected by a thermostat.

For the polymer chain, we also calculate the dynamic structure factor $S(k, t)$, which in physical systems can be measured by dynamic light scattering experiments⁴⁵

$$S(k, t) = \frac{1}{N} \sum_{ij} \left\langle \frac{\sin[k|\mathbf{r}_i(t_0 + t) - \mathbf{r}_j(t_0)|]}{k|\mathbf{r}_i(t_0 + t) - \mathbf{r}_j(t_0)|} \right\rangle_{t_0} \quad (11)$$

where N is the monomer-length of the chain, k is the magnitude of the scattering vector (with units of nm^{-1} here), and $\mathbf{r}_i(t)$ is the position of monomer i . The magnitude of the scattering vector as well as the molecule's radius of gyration R_g determines the types of motion that may be detected, with translational motion dominating when $kR_g \ll 1$ and internal modes of motion becoming important for $kR_g > 1$. Given our objective of studying the internal dynamics of the polymer and the $R_g \approx 0.7$ nm observed for our model polymer, we use a scattering vector $k = 2.0\sigma^{-1}$, which corresponds to the desired $kR_g > 1$ regime. Additionally, inspection of the log-log plot of the static structure factor $S(k, t = 0)$ vs k revealed that $k = 2.0\sigma^{-1}$ was in the linear region corresponding to the dynamic scaling regime.

We calculate $S(k, t)$ from $t = 0$ to 1000 ps, which for our model polymer is sufficient time for the function to decay to 0 under any type of temperature control. This decay occurs over much longer time scales in other dilute polymer systems.⁴⁶ The rapid decorrelation observed here may be attributed to the high flexibility of our model polymer, which as mentioned does not include bending or torsional terms.

We aim to quantify the rate of decorrelation to compare the effects of the various thermostats. It has been found previously,⁴⁶ and we also observed here that $S(k, t)$ in the $kR_g > 1$ regime cannot be accurately described by a single exponential function but that a stretched exponential is often appropriate. We therefore fit the data with a stretched exponential function of the form $y = A \exp(-(t/\tau_B)^C)$ and measure a characteristic decorrelation rate as τ_B^{-1} . For a given thermostat, we determine the mean $S(k, t)$ by averaging the

functions of the 15 independent simulations and the overall decorrelation rate by fitting the resulting function. The associated errors were estimated by bootstrapping the standard deviation of the mean function and its associated decorrelation rate, again with 1000 bootstrap samples.

4. RESULTS AND DISCUSSION

4.1. Bulk Water Dynamics. Throughout this section we refer to the Andersen thermostat, the massive Andersen variant, and Langevin dynamics as “velocity randomizing” algorithms and classify the Berendsen thermostat, Bussi and co-workers’ stochastic velocity rescaling thermostat, and the Nosé-Hoover thermostat as “velocity scaling” algorithms. We first consider how the dynamics of the pure water system are affected by these six thermostats as well as by other schemes which illustrate different factors that can dampen dynamics in general. With this system we investigate dynamic processes that occur on relatively short time scales, by considering the self-diffusivity, rotational correlation time, and shear viscosity of water.

Figure 1 shows these transport properties obtained from NVT simulations using various thermostats and coupling strengths τ_T . It is clearly evident that the velocity randomizing thermostats significantly dampen the dynamics of the fluid as compared to the NVE results, particularly with strong coupling. As previously mentioned, the NVE simulation is used as a benchmark for comparing the various thermostats, because in the NVE ensemble a system evolves according to the “true” Newtonian equations of motion. With the massive Andersen algorithm coupled with $\tau_T = 0.1$ ps, the self-diffusion of water is slower by approximately a factor of 4, and the characteristic time for rotation and shear viscosity are increased by factors of 2. With the traditional Andersen thermostat and Langevin dynamics, the dampening effects are less severe but still significant. These effects diminish as the coupling strength of the velocity randomizing thermostat weakens, and at $\tau_T = 10$ ps the properties agree, within error, with those of the NVE simulation. It is interesting to note that with both the conventional and massive implementation of the Andersen algorithm, each particle’s velocity is randomized on average at the same frequency, yet the massive Andersen method leads to greater dampening of the dynamics for TIP3P water and for the

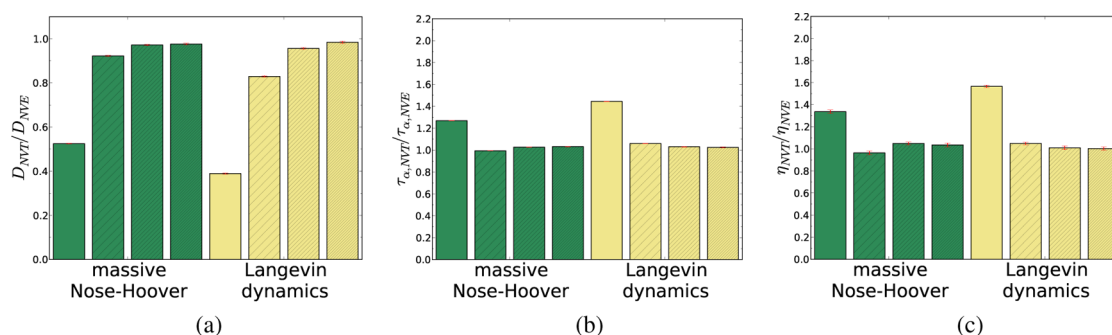


Figure 2. Self-diffusivity (a), rotational correlation time (b), and shear viscosity (c) of pure TIP3P water using massive Nosé-Hoover coupling and Langevin dynamics temperature control with various coupling strengths: $\tau_T = 0.1$ ps (no lines), $\tau_T = 1$ ps (slanted lines, thin space), $\tau_T = 10$ ps (slanted lines, thinner space), and $\tau_T = 100$ ps (slanted lines, thinnest space). Both thermostat algorithms significantly dampen the dynamics when applied with strong coupling.

other systems as well. This may be because τ_T represents the average time between randomizations, and thus with the conventional method there are a large number of particles that continue uninterrupted trajectories for longer than τ_T .

On the other hand, the velocity scaling algorithms--Berendsen, stochastic rescaling, and Nosé-Hoover--yield properties that agree with the NVE values, regardless of τ_T , down to 0.1 ps. This is true even with stochastic velocity rescaling, as has been shown previously for other systems.¹³ The thermostat's stochastic component does not influence particle velocities directly, and their natural time correlations are generally preserved. Our results using the velocity scaling thermostats and NVE are consistent with previous studies of pure water systems.^{43,47,48}

As previously mentioned, dampened dynamical properties are evidence of disruptions to the time correlations of velocities throughout the system and/or over an extended time. The above results for the Andersen methods and Langevin dynamics agree with many previous observations that randomization of velocities leads to dampened dynamics.^{10,11} Velocity rescaling algorithms also may affect velocity time correlations, and therefore dynamical properties, if they lead to large changes in the velocities at each step. As mentioned, this is a possibility using a massive temperature coupling scheme in which each particle is independently coupled to its own thermostat, which is in turn coupled to the rapidly fluctuating kinetic energy of that same particle.

To determine if such a scheme could appreciably affect velocities, such that ensemble-averaged dynamics are dampened, we ran additional simulations of the pure water system subjected to massive Nosé-Hoover coupling. An independent Nosé-Hoover thermostat (with a single Nosé-Hoover chain) was applied to each particle using the same τ_T and $T_0 = 300$ K for each thermostat. The Nosé-Hoover masses were chosen to be proportional to the number of degrees of freedom that they couple to (in this case $N_f = 3$), as suggested by Martyna et al.¹⁶ Harmonic bonds with a time step of 0.5 fs were required to implement this scheme for TIP3P water in GROMACS, in contrast to the explicit constraints and 2 fs time step used for the other simulations, because holonomic constraints are not preserved when different atoms in the constraint system are scaled by different amounts. This treatment of bonds changes slightly the magnitude of the transport properties, and therefore we normalize the massive Nosé-Hoover results by the properties obtained from NVE simulations with harmonic bonds and compare to the NVE-normalized results obtained

using the thermostats with constraints. Deviations from unity reflect the extent to which a given thermostat dampens a property relative to the NVE dynamics.

Figure 2 shows the normalized transport properties using the massive Nosé-Hoover scheme as well as Langevin dynamics, a thermostat which we found significantly affects the dynamics. As shown, the massive Nosé-Hoover with strong coupling does indeed dampen the dynamics, slowing diffusion by nearly a factor of 2 when $\tau_T = 0.1$ ps. This shows that dampening due to a massive implementation of a velocity scaling algorithm can be comparable to that of a velocity randomizing thermostat. The difference between the massive and global Nosé-Hoover schemes is significant, though it is not clear exactly to what extent this is because individual kinetic energies fluctuate more than the global kinetic energy or because the thermostat masses Q_i are smaller in the massive scheme. It is possible that similar effects would be observed with massively coupled Berendsen and stochastic rescaling thermostats, though implementation issues in GROMACS prevent directly testing this hypothesis at this time.

For massive Nosé-Hoover and Langevin dynamics, we conducted additional simulations with $\tau_T = 100$ ps to determine how the dynamics are affected with very weak temperature coupling. In this limit, both schemes yield dynamical properties that converge to within 2% of the NVE results. At this τ_T the thermostats also maintain the average instantaneous temperature at the target $T_0 = 300$ K (within statistical error) as effectively as they do with stronger coupling. Therefore, even algorithms known to dampen dynamics with strong coupling can be used in constant temperature simulations in which relatively short time scale dynamics are important, if one uses a sufficiently weak τ_T that only negligibly impacts the velocity time correlations. However, it is possible that dynamical processes occurring in more complex systems and/or on longer time scales would be more sensitive to velocity randomization or massive velocity rescaling, even when weakly coupled. We note that with the Nosé-Hoover approach, the value of τ_T depends on exactly how the heat bath variable Q is defined. Different multiplicative factors of the product $\tau_T^2 T_0$ are sometimes used,^{8,19} which affects the fictitious mass coupled to a given particle and therefore the magnitude of changes made to the particle's velocities. We can, however, say that as the coupling becomes stronger, the dynamics will begin to diverge from the NVE dynamics.

The consistent dampening effects of the Andersen, massive Andersen, and Langevin dynamics algorithms clearly show that

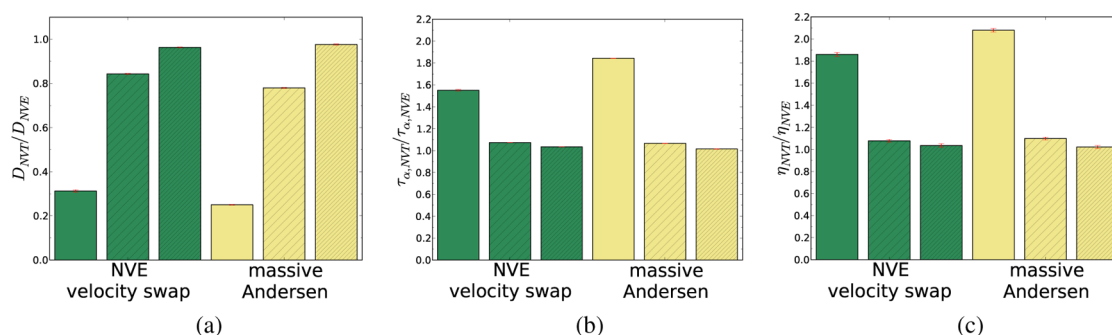


Figure 3. Self-diffusivity (a), rotational correlation time (b), and shear viscosity (c) of pure TIP3P water obtained from NVE simulations in which velocities are swapped at intervals of τ_T and from NVT simulations with massive Andersen temperature control. The coupling strengths are as follows: $\tau_T = 0.1$ ps (no lines), $\tau_T = 1$ ps (slanted lines, thin space), $\tau_T = 10$ ps (slanted lines, thinner space). The deterministic and the stochastic reassignment algorithms significantly dampen the dynamics in a similar way when applied with strong coupling.

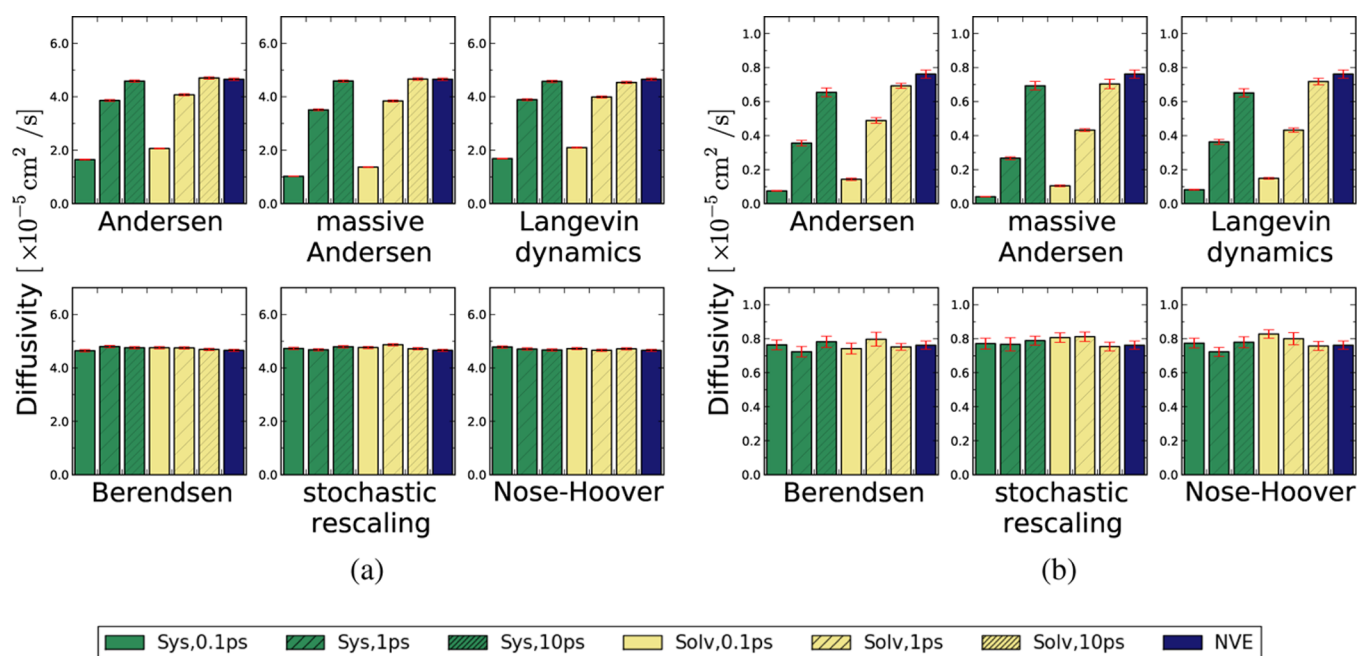


Figure 4. Diffusivities of solvated united-atom methane (a) and solvated polymer chain (b) with thermostats applied to either the entire system (Sys) or to only the solvent (Solv). Velocity randomizing thermostats (upper figures) with strong coupling ($\tau_T = 0.1$ ps) increase the self-diffusivity of water and the diffusivities of both solutes tested, with a larger effect observed for the polymer. The noninvasive scheme of coupling only the solvent slightly reduces the damping of diffusion.

the reassignment of particle velocities disturbs their time correlations. “Randomness” per se is not required, as shown in Figure 3. Here we plot normalized properties from simulations conducted in the NVE ensemble, in which the velocities of half the molecules in the system are swapped with the velocities of the other half of the molecules (the same ones each time) at regular intervals specified by τ_T . This “NVE velocity-swap” scheme does not control the temperature at all but serves as a deterministic velocity randomization scheme, as the velocity reassigned to a given particle comes from another particle within the system. Figure 3 shows that this scheme leads to a dampening of dynamics comparable to that of its stochastic analog, the massive Andersen thermostat. It is the reassignment of the particles with velocities uncorrelated to their previous velocities that leads to the slowed dynamical properties, not “randomization” per se.

These simulations of a pure fluid system illustrate various properties of a thermostat which can lead to artifacts in the dynamics. Direct alteration of velocities, whether by stochastic

or deterministic reassignment or by the use of stochastic forces, significantly dampens dynamical processes occurring on short time scales. Comparable effects are observed with velocity scaling algorithms if implemented locally, such that individual particles’ velocities change rapidly as a function of time. The effects of both of these factors diminish in the limit of weak coupling, which corresponds to infrequent randomizations or slow relaxation of the kinetic energy to its target, for velocity randomizing or rescaling algorithms, respectively.

4.2. Solute Dynamics. We restrict the following study of solute dynamics to the six standard thermostats listed above, with the velocity rescaling algorithms applied globally. While the thermostats are classified as either velocity randomizing or rescaling algorithms, we emphasize that these classes do not necessarily lead to dampened and correct dynamics, respectively, but that the effects of a given algorithm will depend on the way in which it is applied.

Figure 4 shows the translational diffusivities for the solvated UA-methane and polymer chain using various types of

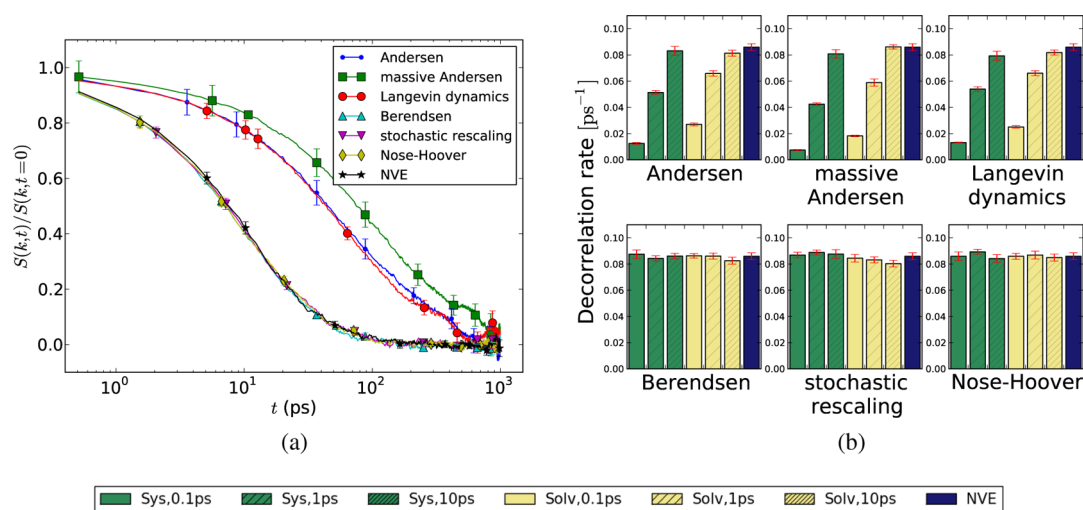


Figure 5. Dynamic structure factor $S(k,t)$ of solvated polymer chain with various thermostats applied to the entire system with $\tau_T = 0.1$ ps (a). Velocity randomizing algorithms lead to polymer structures that remain correlated over longer times. The rate of decorrelation, as measured by the time constant of a stretched exponential fit to $S(k,t)$, is shown for all temperature control schemes tested (b). The magnitude of scattering vector is $k = 2.0\sigma^{-1}$ for all $S(k,t)$ reported.

temperature control. With these systems we also compare the “system-wide” scheme of applying a single thermostat uniformly to the entire system versus the noninvasive approach of applying the thermostat only to the solvent. Similar to our results for the self-diffusion of water, we see that, in general, solute diffusion is slowed by the velocity randomizing thermostats with strong coupling as compared to the NVE results but is unaffected by the velocity scaling methods regardless of the coupling strength. The strategy of coupling only the solvent particles slightly mitigates the dampening of diffusion observed with velocity randomizing algorithms. For example, using Langevin dynamics and $\tau_T = 0.1$ ps, the noninvasive scheme increases the diffusivities of UA-methane and the polymer by 25% and 90% as compared to the system-wide scheme, though even with this increase the diffusivities are well below the NVE results. This suggests that velocity randomization of the solvent particles dampens not only the solvent dynamics but also the dynamics of the solute in thermal contact with the thermostatted solvent. Therefore, regardless of which degrees of freedom are coupled, when such an algorithm is used it is important to choose an appropriately weak τ_T if the correct solute dynamics are to be preserved.

We also observe that the dampening of UA-methane’s diffusion is comparable to the dampening of the self-diffusion of water, while diffusion of the larger polymer molecule is dampened more significantly. Using Langevin dynamics applied to the entire system with $\tau_T = 0.1$ ps, the polymer’s diffusivity is lower than the NVE result by approximately 90%, while the diffusivities of both pure TIP3P water and UA-methane are lower than their respective NVE results by approximately 60%. Using system-wide Langevin dynamics and weak coupling of $\tau_T = 10$ ps, the polymer’s diffusivity is still approximately 15% lower than the NVE value, though it approaches to the NVE result (within error) when coupling is applied only to the solvent. This suggests there is a relationship between a molecule’s size and the extent to which velocity randomization affects its translational diffusion. Therefore, when using a velocity randomizing algorithm to simulate a large solute at constant temperature, very weak coupling and possibly relaxing or removing temperature coupling to the solvent may be

necessary to obtain the correct translational diffusion. It is possible that the sensitivity of other dynamical properties to velocity randomization also depends on the solute size.

The polymer dynamic structure factor $S(k,t)$ describes a dynamic process which occurs on longer time scales, the fluctuations of the chain’s structure. Figure 5a shows representative $S(k,t)$ functions for NVE and NVT simulations, the latter with various thermostats applied to the entire system with $\tau_T = 0.1$ ps. The scattering vector $k = 2.0\sigma^{-1}$ is appropriate for detecting internal motions of the chain, as $kR_g > 1$. As shown, the rate of decay of $S(k,t)$ is much slower with velocity randomizing thermostats than with velocity scaling thermostats or NVE. The former methods slow down the natural configurational fluctuations in the chain, leading to structures that remain correlated over times of up to 1 ns. As previously discussed, these time scales are much less than those observed in other polymer simulations and in experiments, due to the high flexibility of our model chain. As a check we calculated another dynamic property of the polymer, the autocorrelation function of the end-to-end distance of the chain, and found that it decays on time scales of the same order of magnitude as $S(k,t)$. Despite the generally rapid fluctuations of our model chain, the impact of velocity randomizing thermostats on the collective internal dynamics of a polymer is evident with this simplified model. We note that there is good agreement in our results obtained using the Berendsen and Nosé-Hoover thermostats, whereas Lingenheil and co-workers observe dampened peptide dihedral transitions under Berendsen control.²¹ One possible interpretation is that the conformational fluctuations of our model polymer chain involved barriers that are low enough to be crossed with the kinetic energy fluctuations observed using Berendsen temperature control, while the dihedral barriers observed by Lingenheil et al. were not, but resolving that question is beyond the scope of the current study.

Upon fitting $S(k,t)$ with the stretched exponential $y = A \exp(-(t/\tau_B)^C)$ we find that the parameters A and C vary little (<10%) with respect to the type of thermostat, but there are significant deviations in the time constant τ_B . Using τ_B^{-1} to quantify the rate at which the chain’s structure decorrelates, we

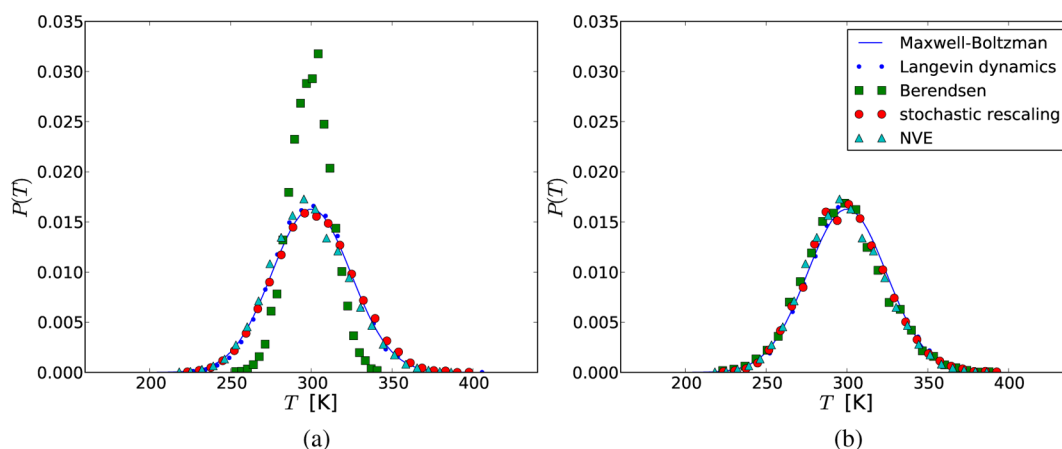


Figure 6. Distribution of the polymer chain's instantaneous temperature with (a) temperature coupling applied to the whole system and (b) coupling applied to only the solvent. A canonical kinetic energy distribution for the polymer can be obtained even with NVE if the solvent bath is sufficiently large and with Berendsen if only the solvent is thermostatted, as the solvent acts as a thermal bath for which only the average temperature is important.

compare the dynamics with various temperature coupling schemes in Figure 5b. Again we observe a dampening effect of slower decorrelation rates due to velocity randomizing thermostats, which is mitigated somewhat by using weaker coupling and coupling only the solvent. Decorrelation rates obtained using the global velocity scaling algorithms agree with the NVE result, within error. The corresponding characteristic decorrelation time τ_B varies from 10 ps with velocity scaling temperature control and NVE, to approximately 80 and 140 ps with strongly coupled Langevin dynamics and the massive Andersen thermostat, respectively.

It is possible that the dynamics of different modes of motion could exhibit varying sensitivities to a thermostat which disrupts velocity time correlations, though the differences we observe for our model polymer chain may be of limited practical significance. Whereas the polymer's translational diffusion using Langevin dynamics and $\tau_T = 1$ ps is approximately 50% slower than with NVE, its structure factor decorrelation rate, which reflects higher order modes of motion, is only 15% lower than the NVE result. In principle, this suggests that when using a thermostat that can potentially decorrelate velocities, the appropriate coupling strength depends on the time scale of the dynamic process of interest. However, differences between the τ_T values needed to obtain accurate results for one dynamic process versus another might be too small to justify careful study of these parameters for various systems, in which case the conservative choice of a weak coupling strength would ensure that all dynamics are relatively well-preserved.

4.3. Temperatures and Energy Distributions. Because the thermodynamics of a system are important in and of themselves and can influence kinetic processes as well, we measure the effects of the various thermostats on the average and distribution of the polymer chain's instantaneous temperature. The average temperature of the polymer is maintained at or near the target $T_0 = 300$ K by all the thermostats tested, for both the approaches of coupling the entire system and coupling only the solvent. The Andersen thermostats with strong coupling and the Nosé-Hoover thermostat with any τ_T provide the most precise and accurate temperature control, with deviations from T_0 of less than 0.1 ± 0.01 K. Precise control is also obtained with the Berendsen thermostat, stochastic velocity rescaling, and Langevin dynamics when strongly

coupled; however, deviations of up to 1 ± 0.1 K are observed using Berendsen and stochastic velocity rescaling with $\tau_T = 10$ ps. These small but statistically significant deviations may be a result of artifacts observed by Lingenheil et al.²¹ and may point to issues using thermostats with a single bath. With coupling applied only to the solvent, larger deviations of up to 2 ± 1 K are observed with some algorithms; however, as seen in Figures 4b and 5b, these variations are not statistically significant enough to appreciably affect the polymer dynamics tested here. Average temperatures for the pure solvent and solvated small molecule systems are similarly well-controlled.

As previously mentioned, an incorrect energy distribution can impact certain dynamic processes. We therefore compare the distributions of the polymer's instantaneous temperature from our simulations to the predicted distribution for the true canonical ensemble. To calculate this prediction, we first note that for a system with kinetic energy $(3N)/(2k_B T)$, the associated variance is $\sigma_{KE}^2 = k_B T^2 C_V$. If one considers only the kinetic energy, the ideal gas heat capacity may be used for C_V , which yields a kinetic energy variance of $\sigma_{KE}^2 = (3N)/(2(k_B T)^2)$. We find the temperature corresponding to this σ_{KE} by noting that, on average, $KE = (3/2)Nk_B T$. Finally, because N of our polymer chain is sufficiently large, we approximate the Maxwell-Boltzmann distribution as a Gaussian with mean $T = 300$ K and standard deviation $\sigma_T = (2\sigma_{KE})/(3Nk_B)$.

In Figure 6 we compare this analytic distribution to those obtained from the simulations with system-wide and solvent-only temperature coupling, respectively. We also include the NVE distribution. Figure 6a shows that when the Berendsen thermostat is applied to the entire system with strong coupling, the polymer chain samples an overly narrow distribution of temperatures (and therefore kinetic energies). In more complex systems, this could be reflected in dampened kinetics for processes that depend on large energy fluctuations.²¹ On the other hand, Langevin dynamics and stochastic velocity rescaling yield distributions that reflect the true canonical ensemble, and the NVE simulation deviates only slightly from the canonical prediction.

Figure 6b shows the polymer temperature distributions when only the solvent is thermostatted. Slight deviations in the peak locations reflect the previously discussed variations in the mean. In general, the results match the Maxwell-Boltzmann

distribution for all NVT simulations as well as for NVE. Agreement with the canonical distribution even in the absence of direct thermostating supports previous findings that a solvent may effectively control a solute's temperature by virtue of its thermal contact with the molecule, acting as a heat bath.²¹ This is true even for the Berendsen thermostat, which does not give the proper distribution when applied to the entire system. However, in the standard derivation of the canonical distribution, all that is required of the heat bath is that it be much larger than the system and that its temperature is fixed, conditions that are met with Berendsen coupled to the solvent and also with no coupling (NVE) if the solvent bath is sufficiently large. In some cases an explicit thermostat, rather than just a large solvent bath at NVE, might be necessary to avoid significant drift in the solute temperature over long times, though if the integration is sufficiently accurate, the solute heating time scale should be much longer than the time scale of heat transport between the solute and solvent.

5. CONCLUSIONS

A variety of methods have been developed to run isothermal molecular dynamics simulations. These algorithms modify either the equations of motion or the particle velocities directly and therefore can have unintended effects on the system's dynamics and thermodynamics. We have compared how six different thermostats and various coupling schemes influence these aspects of a simulation, particularly the dynamics as measured by fundamental transport properties.

The dampening of dynamical properties reflects systemic decorrelation of particle velocities due to factors external to the molecular description itself, in this case a thermostat algorithm. As one would expect, velocity time correlations are disrupted by thermostats that randomize velocities. These include the Andersen thermostat, which stochastically reassigns velocities at regular intervals, and Langevin dynamics, which includes additional terms for stochastic noise and friction in the equations of motion. When these algorithms are applied with strong coupling, we find the dynamics are significantly dampened relative to the NVE results, which provide a measure of the true dynamics obtained with the unaltered equations of motion. The dampening effects are observed in dynamics measured over various time scales, including shear viscosities (10^0 – 0^1 ps time scale), translational and rotational diffusion (10^0 – 10^1 ps), and the dynamic structure factor of the polymer (10^0 – 10^3 ps for our model). We find that a massive Andersen approach generally leads to greater dampening of dynamics than the conventional Andersen thermostat, despite reassigning velocities at the same rate, and that a deterministic reassignment strategy leads to similar effects as those observed with Andersen, which uses stochastic reassignment.

For solvated molecules, the dampening of dynamics is only somewhat mitigated by the noninvasive strategy of applying the thermostat to the solvent only. This suggests that a solute's diffusion and higher-order dynamics can be slowed just by virtue of its thermal contact with a solvent subjected to velocity randomization. In general, the effects of a velocity randomizing thermostat diminish as the coupling strength weakens, approaching the Newtonian dynamics limit if coupling times are on the order of 10 ps for these systems. We also observe that the extent to which these methods slow a solute's diffusion increases with the size of the molecule and that the extent to which they dampen a given transport property depends on the time scale of the dynamical process. Translational diffusion of

our model polymer was slowed more significantly by velocity randomization than was the decorrelation rate of the polymer's dynamic structure factor.

Algorithms which operate by scaling particle velocities include the Berendsen thermostat and Bussi and co-workers' stochastic velocity rescaling thermostat, which adjust velocities so that the temperature relaxes exponentially to its target at a specified rate, and the Nosé-Hoover thermostat, which adjusts velocities by coupling the equations of motion to extended dynamical variables and gives an oscillatory relaxation to the target. When applied globally to the system using any coupling strength, these thermostats yield transport properties that are statistically indistinguishable from the NVE results. However, a massive implementation of the Nosé-Hoover thermostat, in which each particle is coupled independently to its own thermostat, leads to dampening on the same order as that observed using Langevin dynamics. This illustrates that even a velocity scaling algorithm can significantly disturb velocity time correlations if the scalings are sufficiently large, for instance if particles are coupled to their own rapidly fluctuating kinetic energies with light masses.

It appears that the well-documented problem of the Berendsen thermostat providing an incorrect distribution of instantaneous temperature may be largely mitigated by applying the thermostat to only the solvent, as long as one is only concerned with the dynamics of the solvated system. In more complex systems with kinetic processes that depend on energy fluctuations, this approach could possibly preserve the correct dynamics. However the same results might be obtained with stochastic velocity rescaling or the Nosé-Hoover thermostat, without the need to remove the coupling of the solute.

These findings suggest that velocity scaling methods are most appropriate for simulations that require both constant temperature and realistic dynamics. When applied globally, as is typically done, these thermostats yield correct transport properties which describe processes that occur on relatively short time scales. However, these algorithms do not intrinsically preserve the correct dynamics; if applied to local kinetic energies they can lead to dampening effects comparable to those caused by velocity randomizing thermostats, unless the coupling is sufficiently weak.

We find that the globally applied stochastic rescaling and Nosé-Hoover thermostats are particularly effective in preserving the correct transport properties and thermodynamic distributions. Velocity randomizing algorithms should be used with caution when accurate representations of dynamical processes are important; even if the dynamics are not important, they will slow down the rate of sampling for the system. However, their dampening effects may be reduced by using a sufficiently weak coupling strength or a noninvasive coupling strategy, provided the temperature is adequately controlled. Even when the dynamics of a system are important, these methods might be useful depending on the objective. For example, in an implicit solvent simulation, stochastic velocity randomization serves to model the thermal collisions of the omitted solvent molecules, and the coupling strength can be tuned to yield a desired solute diffusivity.

It is important to note that this study only examined subnanosecond kinetics. It remains an open question if lessons learned here also extend to longer time scale collective dynamics. It could be that over the nanosecond or microsecond time scales important in protein folding, velocity scaling algorithms will also have dampening effects that cannot be

detected in the simulations performed here, or alternatively that the distortions of the fast kinetics are unimportant to much longer dynamical processes that simply require sufficiently large fluctuations in the local kinetic energy to activate. However, given the absence of any statistically noticeable effect of these algorithms on short time scale kinetics, it is likely worth testing the hypothesis that these integrators do not significantly affect dynamics on longer time scales.

In summary, we have shown how the fundamental molecular dynamics practice of controlling the temperature can modify the dynamics and transport properties in simulations of simple test systems. Improving our understanding of these effects, particularly for more complex systems, is an important step toward correctly choosing thermostats in order to obtain the best estimates of the properties desired from the simulation.

■ ASSOCIATED CONTENT

■ Supporting Information

Tables S1–S3 give the results for the self-diffusivity, rotational correlation time, and shear viscosity of the pure TIP3P water system shown in Figure 1. Tables S4 and S5 give the translational diffusion results for the UA methane and polymer chain systems, shown in Figure 4. Table S6 gives the results for the decorrelation rate of the dynamic structure factor of the polymer chain shown in Figure 5b. This material is available free of charge via the Internet at <http://pubs.acs.org>.

■ AUTHOR INFORMATION

Corresponding Author

*E-mail: michael.shirts@virginia.edu.

Notes

The authors declare no competing financial interest.

■ ACKNOWLEDGMENTS

This work was supported in part by the U.S. National Science Foundation (Grant No. CBET-1032727). The authors acknowledge Lillian T. Chong and Daniel M. Zuckermann for useful discussions.

■ REFERENCES

- (1) Berger, O.; Edholm, O.; Jähnig, F. *Biophys. J.* **1997**, *72*, 2002–2013.
- (2) Snow, C. D.; Nguyen, H.; Pande, V. S.; Gruebele, M. *Nature* **2002**, *420*, 102–106.
- (3) Cadena, C.; Zhao, Q.; Snurr, R. Q.; Maginn, E. J. *J. Phys. Chem. B* **2006**, *110*, 2821–2832.
- (4) Zhang, L.; Greenfield, M. L. *J. Chem. Phys.* **2007**, *127*, 194502.
- (5) Fan, H.; Mark, A. E. *Protein Sci.* **2004**, *13*, 211–220.
- (6) Hünenberger, P. H. In *Advanced Computer Simulation*, Holm, C., Kremer, K., Eds.; *Adv. Polym. Sci.*; Springer: Berlin, Heidelberg, 2005; Vol. 173; pp 105–149.
- (7) Shirts, M. R. *J. Chem. Theory Comput.* **2013**, *9*, 909–926.
- (8) Hess, B.; Kutzner, C.; van der Spoel, D.; Lindahl, E. *J. Chem. Theory Comput.* **2008**, *4*, 435–447.
- (9) Andersen, H. C. *J. Chem. Phys.* **1980**, *72*, 2384–2393.
- (10) Frenkel, D.; Smit, B. *Understanding Molecular Simulation: From Algorithms to Applications*; Academic Press: 2002.
- (11) Bussi, G.; Parrinello, M. *Comput. Phys. Commun.* **2008**, *179*, 26–29.
- (12) Berendsen, H. J. C.; Postma, J. P. M.; van Gunsteren, W. F.; DiNola, A.; Haak, J. R. *J. Chem. Phys.* **1984**, *81*, 3684–3690.
- (13) Bussi, G.; Donadio, D.; Parrinello, M. *J. Chem. Phys.* **2007**, *126*, 014101.
- (14) Nosé, S. *J. Chem. Phys.* **1984**, *81*, 511–519.
- (15) Hoover, W. G. *Phys. Rev. A* **1985**, *31*, 1695–1697.
- (16) Martyna, G. J.; Klein, M. L.; Tuckerman, M. *J. Chem. Phys.* **1992**, *97*, 2635–2643.
- (17) Harvey, S. C.; Tan, R. K. Z.; Cheatham, T. E. *J. Comput. Chem.* **1998**, *19*, 726–740.
- (18) Mudi, A.; Chakravarty, C. *Mol. Phys.* **2004**, *102*, 681–685.
- (19) Tobias, D. J.; Martyna, G. J.; Klein, M. L. *J. Phys. Chem.* **1993**, *97*, 12959–12966.
- (20) Morrone, J. A.; Car, R. *Phys. Rev. Lett.* **2008**, *101*, 017801.
- (21) Lingenheil, M.; Denschlag, R.; Reichold, R.; Tavan, P. *J. Chem. Theory Comput.* **2008**, *4*, 1293–1306.
- (22) Weber, W.; Hünenberger, P. H.; McCammon, J. A. *J. Phys. Chem. A* **2000**, *104*, 3668–3675.
- (23) Cuthbertson, J. M.; Bond, P. J.; Sansom, M. S. P. *Biochemistry* **2006**, *45*, 14298–14310.
- (24) Tao, Y.; Rao, Z.-H.; Liu, S.-Q. *J. Biomol. Struct. Dyn.* **2010**, *28*, 143–157.
- (25) Gallo, M. T.; Grant, B. J.; Teodor, M. L.; Melton, J.; Cieplak, P.; Phillips, G. N. J.; Stec, B. *Mol. Simul.* **2009**, *35*, 349–357.
- (26) Leimkuhler, B.; Noorizadeh, E.; Penrose, O. *J. Stat. Phys.* **2011**, *143*, 921–942.
- (27) Groot, R. D.; Warren, P. B. *J. Chem. Phys.* **1997**, *107*, 4423–4435.
- (28) Goga, N.; Rzepiela, A. J.; de Vries, A. H.; Marrink, S. J.; Berendsen, H. J. C. *J. Chem. Theory Comput.* **2012**, *8*, 3637–3649.
- (29) Lowe, C. P. *Europhys. Lett.* **1999**, *47*, 145–151.
- (30) Pastorino, C.; Kreer, T.; Müller, M.; Binder, K. *Phys. Rev. E* **2007**, *76*, 026706.
- (31) Fuzo, C. A.; Degreve, L. *J. Mol. Model.* **2012**, *18*, 2785–2794.
- (32) Rosta, E.; Buchete, N.-V.; Hummer, G. *J. Chem. Theory Comput.* **2009**, *5*, 1393–1399.
- (33) Spill, Y. G.; Pasquali, S.; Derreumaux, P. *J. Chem. Theory Comput.* **2011**, *7*, 1502–1510.
- (34) Ryckaert, J. P.; Ciccotti, G.; Berendsen, H. J. C. *J. Comput. Phys.* **1997**, *23*, 327–341.
- (35) Andersen, H. C. *J. Comput. Phys.* **1983**, *52*, 24–34.
- (36) Jorgensen, W. L.; Tirado-Rives, J. *J. Am. Chem. Soc.* **1988**, *110*, 1657–1666.
- (37) Martin, M. G.; Siepmann, J. I. *J. Phys. Chem. B* **1998**, *102*, 2569–2577.
- (38) Bjelkmar, P.; Larsson, P.; Cuendet, M. A.; Hess, B.; Lindahl, E. *J. Chem. Theory Comput.* **2010**, *6*, 459–466.
- (39) Swope, W. C.; Andersen, H. C.; Berens, P. H.; Wilson, K. R. *J. Chem. Phys.* **1982**, *76*, 637–649.
- (40) Hockney, R. W.; Goel, S. P.; Eastwood, J. J. *Comput. Phys.* **1974**, *14*, 148–158.
- (41) Allen, M. P.; Tildesley, D. J. *Computer Simulation of Liquids*; Oxford Science Publications: 1987.
- (42) Chitra, R.; Yashonath, S. *J. Phys. Chem. B* **1997**, *101*, 5437–5445.
- (43) van der Spoel, D.; van Maaren, P. J.; Berendsen, H. J. C. *J. Chem. Phys.* **1998**, *108*, 10220–10230.
- (44) Hess, B. *J. Chem. Phys.* **2002**, *116*, 209–217.
- (45) Binder, K. *Monte Carlo and Molecular Dynamics Simulations in Polymer Science*; Oxford University Press: 1995; pp 125–194.
- (46) Harnau, L.; Winkler, R. G.; Reineker, P. *J. Chem. Phys.* **1996**, *104*, 6355–6368.
- (47) Yeh, I.-C.; Hummer, G. *J. Phys. Chem. B* **2004**, *108*, 15873–15879.
- (48) Mark, P.; Nilsson, L. *J. Phys. Chem. A* **2001**, *105*, 9954–9960.